Genome Sequencing-based Coverage Analyses Facilitate High-resolution Detection of Causal Deletions in Gamma-Irradiated Wheat Mutants

Shoya Komura
Graduate School of Agricultural Science, Kobe University
Hironobu Jinno
Kitami Agricultural Experiment Station, Hokkaido Research Organization
Tatsuya Sonoda
Kitami Agricultural Experiment Station, Hokkaido Research Organization
Yoko Oono
Institute of Crop Science, National Agriculture and Food Research Organization
Hirokazu Handa
Institute of Crop Science, National Agriculture and Food Research Organization
Shigeo Takumi
Graduate School of Agricultural Science, Kobe University
Kentaro Yoshida (kentaro.yoshida.plg@gmail.com)
Graduate School of Agricultural Science, Kobe University
Fuminori Kobayashi
Institute of Crop Science, National Agriculture and Food Research Organization

Research Article

Keywords: Hexaploid wheat, gamma-irradiated mutant, whole genome sequencing, grain hardness, pre-harvest sprouting tolerance

Posted Date: June 1st, 2021

DOI: https://doi.org/10.21203/rs.3.rs-551628/v1

Abstract

Background

Gamma-irradiated mutants of hexaploid wheat, *Triticum aestivum* L., have been providing novel and agriculturally important traits and are used for breeding materials. However, identification of causative genomic regions of mutant phenotypes was challenging due to the large and complicated genome of hexaploid wheat. Recently, the combined use of high-quality reference genome sequences of common wheat and cost-effective resequencing technologies has made it possible to evaluate genome-wide polymorphisms even in hexaploid wheat.

Results

To investigate whether genome sequencing approach can effectively detect structural variations such as deletions that are frequently caused by gamma irradiation, we selected a grain-hardness mutant from gamma-irradiated population of Japanese elite wheat cultivar “Kitahonami”. It is known that a *Hardness* (*Ha*) locus including puroindoline protein-encoding genes *Pina-D1* and *Pinb-D1* on the short arm of chromosome 5D mainly regulates the grain hardness variation in common wheat. We performed short-read genome sequencings of the wild-type and the grain-hardness mutant, and then aligned their short reads to the reference genome of wheat cultivar “Chinese Spring.” The genome-wide comparisons of depth-of-coverage between wild-type and the mutant detected a ~130 Mbp deletion on the short arm of chromosome 5D in the mutant genome. Molecular markers for this deletion were applied to the progeny populations generated by a crosse between wild-type and the mutant. The large deletion in the region including the *Ha* locus was exactly associated with the mutant phenotype, indicating that genome sequencing approach is powerful and efficient to detect a causal deletion of a gamma-irradiated mutant. We also investigated a pre-harvest sprouting tolerance mutant and identified a 67.8 Mbp deletion on chromosome 3B where Viviparous-B1 and GRAS family transcription factor are located. Co-dominant markers designed to detect the deletion-polymorphism clearly confirmed an association with the low germination rate led to pre-harvest sprouting tolerance.

Conclusions

Short-read-based genome sequencings of gamma-irradiated mutants facilitate the identification of large deletions responsible for mutant phenotypes when combined with segregation analyses in progeny populations. The method we adopted in this study allows the effective application of mutants with agriculturally important traits to breeding with marker-assisted selection.

Background

Mutagenesis by X-rays and gamma irradiation has been widely used to generate mutants in crops [1, 2]. These irradiated mutants have been used as materials for new variety breeding, linkage map construction, and gene function analysis. In wheat, morphological and physiological mutants such as

grain shapes and anthesis are generated by X-rays and gamma irradiation [1]. The mutant plants provide novel and agriculturally useful traits, contributing to wheat breeding as genetic resources. Generation frequency of mutant phenotypes and mutation types are dependent on irradiation dose [1, 3]. Particularly, gamma irradiation often causes structural variations of translocations and inversions on chromosomes and large deletions with chromosomal breakages [1]. Based on the gamma irradiation feature of random occurrence of large deletions, radiation hybrid mapping is developed. Through the assessment of presence or absence of chromosome segments using molecular markers, radiation hybrid mapping allows building the high-resolution maps in wheat and its wild relatives [4, 5]. In addition, causal genetic regions of the phenotypes of the gamma-irradiated wheat mutants are mapped using simple sequence repeat markers in segregating populations derived from crosses between wild-type and the mutants [6].

Development in genome sequencing technology allows to genome-wide genotyping and decoding genome sequences. In maize, the combined bulked segregant RNA-sequencing and exome sequencing approaches are applied to gamma-irradiated maize mutants, successfully identifying causative deletions of the mutant phenotypes [7]. On the other hand, since common wheat (*Triticum aestivum* L.) has a hexaploid species possessing the large and complicated genome with formula AABBDD, it was challenging to apply genome sequencing approach to gamma-irradiated wheat mutants. However, high-quality genome sequence of the common wheat cultivar “Chinese Spring” (CS) has been released [8] and the wheat pangenome project provides ten reference-quality genome assemblies and five scaffold assemblies of common wheat [9]. The presence of the reference genome and the reduction of cost of genome sequencing allow exploring genome-wide polymorphisms even in common wheat, unravelling evolutionary history among cultivated wheat and their wild relatives in high resolution [10]. Now, the application of genome sequencing to common wheat becomes more easily accessible. Genome sequencing of agronomically beneficial mutants generated by gamma irradiation could more efficiently identify causative genomic regions of the mutant phenotypes compared with the classical genotyping approaches.

We developed gamma-irradiated mutants of common wheat cultivar “Kitahonami.” “Kitahonami” is a Japanese winter wheat elite cultivar bred from a cross between the cultivars “Kitami 72” and “Hokushin.” It is adapted to the northern area of Japan and provides high-quality soft grains for the Japanese white salted noodle, udon [11]. If a mutant showing useful agronomic traits is found in the mutant population, it can be used for improving “Kitahonami” as well as other wheat cultivars. We have identified a grain hardness mutant and a pre-harvest sprouting (PHS)-tolerant mutant that were expected to be available for further improvement of wheat cultivars.

Grain hardness of wheat is one of the essential traits to decide grain flour characteristics. A *Hardness* (*Ha*) locus on the short arm of chromosome 5D regulates the grain hardness of common wheat [12]. Allelic differences in two puroindoline genes, *Pina-D1* and *Pinb-D1*, in *Ha* locus cause variations of grain hardness ranging from soft to hard in common wheat [13, 14]. Reduction of gene expression of the *Pina-D1* and *Pinb-D1* genes by the RNAi-mediated gene silencing increases grain hardness in transgenic

common wheat [15, 16], implying that the existence of puroindoline genes is required for forming soft grain in common wheat.

The moist condition provided by precipitation causes PHS in common wheat, a phenomenon of immature seed germination in pre-harvest spikes. PHS gives devastating damages on yields and quality of wheat grains [17, 18, 19, 20]. The beginning of the rainy season in Japan coincides with the wheat harvest time. PHS often occurs when the rainy season begins earlier than as usual. PHS resistance is one of the most essential wheat breeding goals in Japan [21, 22]. PHS is a quantitative trait controlled by multiple genes and is essentially linked to seed dormancy. Several genes associated with seed dormancy and PHS including *MOTHER OF FT AND TEL1* (*MFT1*), *TaMKK3-A*, *Viviparous-B1* (*Vp-B1*), *Qsd1,* and *Tamyb10,* have been identified [23, 24, 25, 26, 27, 28].

In this study, using the grain hardness mutant and the PHS-tolerant mutant, we developed a method to identify causal regions responsible for mutant phenotypes. At first, whole-genome resequencing was applied to these mutants. To detect deleted genomic regions induced by gamma irradiation, we conducted a sliding window analysis of depth-of-coverage over chromosomes. Molecular markers to confirm the causal deletion were designed and applied to the F_2 populations generated by crosses between wild-type and the mutants. Finally, we evaluated how much depth-of-coverage and window size of sliding window analysis were optimal to detect large deletions in gamma-irradiated common wheat. These analyses will provide the good approach to effective breeding methodology using mutants with useful agronomic trait.

Methods

Plant materials

The Japanese elite cultivar “Kitahonami” is a soft winter wheat providing high-quality flour for Japanese white salted noodles. To generate mutants, 250 Gy of gamma-rays were irradiated onto seeds of “Kitahonami.” To screen grain hardness mutants, ~1,200 grains were randomly chosen from the M_2 mutants. The 26 M_2 grains showing amber-color grains were selected. Three individuals showing hard grain characteristics that were estimated by SKCS analysis were selected from the 26 individuals and were regarded as three lines. One line was selected from the three lines in M_4. By repeating selfing of the selected line, the M_7 mutant line, called “30579,” was obtained. For the segregation analysis, F_2 progenies were generated from a cross between “Kitahonami” and “30579” (M_7).

To screen PHS-tolerant mutants, M_2 mutant seeds were randomly selected for M_3 mutants. In the field of Kitami Agricultural Experiment Station, Kitami, Hokkaido, 5,000 M_4 mutants were grown. After flowering, 1,500 spikes were harvested at the maturing stage, sprayed with water in the morning and evening, and incubated at 15 °C for seven days. Seven spikes with low germination and rooting were chosen as PHS-tolerant candidate lines. After M_5 generations, we performed PHS tolerance and seed dormancy tests on every generation, and selected candidate lines showing stronger PHS tolerance and seed dormancy than

the wild-type. In M_7, one candidate line showing stronger PHS tolerance and seed dormancy than the wild-type was selected and named “28511” mutant line. For the segregation analysis, F_2 progenies were generated from a cross between “Kitahonami” and “28511” (M_7).

Tests of grain hardness, PHS tolerance, seed dormancy, and ABA sensitivity

Grain hardness was evaluated using SKCS 4100 (Perten, Stockholm, Sweden). The SKCS hardness index was obtained from crushing a sample of at least 50 kernels each from the wild-type and the grain hardness mutant “30579.”

To test PHS tolerance, spikes were detached during the maturity period after flowering, incubated on trays at 15 ° C, sprayed with water in the morning and evening. After seven days, germination rate and rooting rate were calculated. For the seed dormancy test, 50 seeds 7 days after ripening were incubated in a petri dish at 10 °C or 15 °C. Germination rate was calculated based on the number of germinated seeds after three, five, seven, or nine days.

To test ABA sensitivity, bioassay for ABA responsiveness were performed according to the protocol of Iehisa et al. [50]. Ten seeds of the wild-type or the PHS-tolerant mutant “28511” were treated with running water for six hours. The seeds were incubated on a wet filter paper in a petri dish at 4 °C under dark condition overnight and then incubated at 23 °C for 20 hours. Two petri dishes with filter paper were prepared. Six mL of 20 μM ABA was added to one of the petri dishes, and six mL of ultrapure water was added to the other one as a control. Five germinated seeds were put in each petri dish after measuring root length of the germinated seeds. Root length of each seed was measured 48 hours later. The elongated root length was defined as the difference in root length after 0 hour and 48 hours. The suppression rate of root elongation was calculated by (elongated root length in the ultrapure water – (elongated root length in the ultrapure water – elongated root length in ABA))/elongated root length in the ultrapure water. Three independent bioassays were performed for the wild-type and the PHS-tolerant mutant “28511.”

Extraction of total DNA and genome sequencing

Total DNA was extracted using the CTAB method from the leaves of wild-type and mutant plants of “Kitahonami.” After RNase treatment, PCR-free DNA libraries for 150-bp paired-end DNA sequencing were constructed using TruSeq DNA library Preparation Kit (Illumina, San Diego, CA, USA). DNA sequencings of the wild-type was conducted on Ilumina HiSeq-X sequencer. DNA sequencing of the mutants was performed on NovaSeq sequencer. The sequencing reads were deposited in the database of the Komugi GSP (Genome Sequencing Program) (https://komugigsp.dna.affrc.go.jp/research/download/index.html).

Quality control, Alignments, and SNP calling

Quality of the sequencing reads was checked using FASTQC ver. 0.11.7 [51]. Trimmomatic version 0.33 [52] was used to exclude short reads with an average minimum Phred quality score per four bp of less

than 20 and a length of less than 100 bp. The filtered paired-end reads were aligned to the reference genome of CS version 1.0 [8] using BWA version 0.7.17 [53] with default options. Paired-end reads putatively generated by PCR duplications were removed using SAMtools version 1.9 [54]. The average number of aligned reads and genome coverage of short reads over the reference genome were calculated using BBmap version 37.77 [55]. SNP and indel calling was conducted using bcftools version 1.9 [56]. The command lines used for SNP and indel calling were described in Additional file 1: Table S3. Annotations of SNPs and indels were conducted using SnpEff version 4.3t [57].

Detection of large deletions induced by gamma irradiation

The depth-of-coverage for each genome position was estimated by SAMtools version 1.9. To detect deletions from the distribution of depth-of-coverage over chromosomes, moving average of depth-of-coverage was calculated with a window size of three Mbp and a step size of one Mbp using Python version 3.7.1. The R package ggplot2 was used to visualize the distribution of the moving average of depth-of-coverage, SNP positions, and SNP density over chromosomes. Moving average of differences in depth-of-coverage (Δdepth) between the wild-type and the mutants were also calculated. To estimate 95% confidence interval (q95) and 99% confidence interval (q99), the moving average of depth-of-coverage was randomly extracted from each sample, and Δdepth between the samples was calculated. After this operation was repeated 4,000 times, the top 5% of Δdepth was designated as q95 and the top 1% of Δdepth as q99.

To evaluate how much depth-of-coverage is enough to detect large deletions induced by gamma irradiation, simulations was conducted by subsampling short reads using seqtk version 1.3-r106 [58]. The moving average of depth-of-coverage and Δdepth over chromosomes was calculated and visualized under depth-of-coverage ranging from 2.5x to 15x. Under the 5x depth-of-coverage conditions, simulation of deletion length was conducted by changing deletion length to 40 Mbp, 20 Mbp, 10 Mbp, 5 Mbp, 3 Mbp, and 1 Mbp in four window size conditions, 1 Mbp, 3 Mbp, 5 Mbp, and 10 Mbp.

The command lines, packages, and scripts for the above analyses of deletions were described in Additional file 1: Table S3. The scripts of R and python are available from the Git-Hub repository (https://github.com/ShoyaKomura/WheatGammaIrradiationMutGenomeSeq).

Marker constructions for deletions and deleted genes

The borders of the large deletion in the PHS mutant of “Kitahonami” were estimated based on the distribution of the moving average of depth-of-coverage. The primer was constructed inside the deletion. Two primers were designed outside the deletion. The primers of *Pina-D1* and *Pinb-D1* described in Miki et al. [59] was used to confirm presence/absence of these genes in the wild-type, the grain hardness mutant, and their F_2 progenies. Sequence information of primers for markers and genes are listed in Additional file 1: Table S2. PCR condition of the markers and genes was as follows. After pre-denaturing of 94 °C for 2 minutes, 40 cycles of denaturing of 94 °C for 20 seconds, annealing of 60 °C for 30 seconds, and extension of 68 °C for 30 seconds were conducted, and then post-extension of 68 °C was performed for

one minute. For PCR amplification of the co-dominant marker, the three primers were mixed before application of PCR.

Results

The hard grain mutant of Japanese elite wheat cultivar "Kitahonami"

To confirm the capability of whole-genome resequencing approach to detect large deletions caused by gamma irradiation in the hexaploid wheat, we focused on grain hardness because grain hardness is regulated by *Pina-D1* and *Pinb-D1* genes, loss of which causes the grain hardness change from soft to hard [15, 16]. Given that "Kitahonami" produces soft grains, the hard grain mutant was assumed to have mutations in the *Pina-D1* and *Pinb-D1* regions on the distal region of short arm of chromosome 5D. Based on the grain colour and the Single Kernel Characterization System (SKCS) value, we obtained the grain hardness mutant "30579" from the gamma-irradiated mutant population of "Kitahonami" (Fig. 1). Whereas the SKCS value of the wild-type is 24, the grain hardness of "30579" showed 102 of SKCS value (Table 1). Typically <40 and >70 of SKCS value is regarded as soft and hard grain, respectively. Therefore, the grains of mutant "30579" is hard. Grain protein content was also slightly elevated in the mutant (Table 1). Agronomic characteristics of the mutant "30579" were also compared with those of the wild-type. Grain weight (kg/10a) and 1000-grain weight of the mutant "30579" were low to those of the wild-type, indicating that the yield of the mutant was inferior to that of the wild-type.

Table 1 Agronomic and quality characteristics of "Kitahonami" and the mutant "30579"

	Kitahonami WT	30579
Agronomic characteristics		
Maturity stage (date)[1]	28th July	27th July
Grain weight (kg/10a)	687	578
Ratio (%)	100	84
1000-grain weight (g)	41.2	30.4
Quality characteristics		
Grain Hardness	24	102
Grain protein content (%)	9.4	10.2

[1]Maturity stage was examined in 2019-2020 season.

Comparative genomics of "Kitahonami" and its hard grain mutant "30579" revealed large deletions induced by gamma irradiation

To identify the causal genome region of hard grain of the “Kitahonami” mutant “30579,” genome resequencing of the wild-type and the mutant “30579” were performed. In total, 2.3 to 2.9 billion reads were obtained. After removing short reads with bad quality and PCR duplicates, we obtained 1.8 to 2.3 billion reads aligned to the reference genome of CS (Table 2). Average depth-of-coverage was 15.51 for the wild-type and 18.85 for the mutant. The aligned short reads covered over 94% of the reference genome sequences. The number of single-nucleotide polymorphisms (SNPs) and short indels between “Kitahonami” and CS were 30,597,871 and 1,328,442, while the number of SNPs and short indels between the mutant “30579” and CS were 32,254,934 and 1,713,770.

Table 2 Summary of alignments and coverages of genome sequencing of wild-type and mutants of “Kitahonami”

Name	Total filtered reads (%)[1]	Aligned reads (%)[2]	Aligned reads after removal of PCR duplicate (%)[3]	Reference bases covered (%)	Average depth-of-coverage
Kitahonami	2,736,865,184 (94.05%)	2,732,548,516 (99.84)	2,334,492,027 (85.30%)	95.99	15.51
Kitahonami (5x)[4]	933,526,244 (99.51%)	932,129,013 (99.85%)	876,039,611 (93.84%)	94.38	6.01
30579	2,042,471,104 (87.84%)	2,036,948,509 (99.73%)	1,830,711,894 (89.63%)	94.57	18.85
28511	2,107,121,470 (78.79%)	2,104,170,687 (99.86%)	1,908,476,075 (90.57%)	95.39	19.43
28511 (15x)[4]	1,626,684,636 (78.79%)	1,624,412,275 (99.86%)	1,498,723,901 (92.13%)	95.20	15.35
28511 (10x)[4]	1,084,461,526 (78.79%)	1,082,945,323 (99.86%)	1,025,292,441 (94.68%)	94.86	10.50
28511 (5x)[4]	542,210,918 (78.79%)	541,454,612 (99.86%)	526,465,742 (97.23%)	93.63	5.39
28511 (2.5x)[4]	271,156,212 (78.79%)	270,777,750 (99.86%)	266,912,156 (98.57%)	87.30	2.73

[1] An average base quality score per 4bp >=20

The filtered reads rate = Total filtered reads / Total reads × 100

[2] The aligned reads rate = Aligned reads / Total filtered reads × 100

[3] The filtered reads rate = Aligned reads after removing PCR duplicates / Total filtered reads × 100

[4] The sets of read data were used for the simulations. The number in the paratheses indicates approximate depth-of-coverage.

SNP density distribution over chromosome for the mutant “30579” was almost identical to the wild-type (Fig. 2). The SNP density for the wild-type and the mutant “30579” was unevenly distributed over the chromosomes. In chromosomes 1A, 2A, 1B, 2B, 3B, 5B, and 6B, “Kitahonami” was genetically divergent from CS, while the chromosomes 3A, 4A, 6A, 4B, and 7B were genetically close in the two cultivars, particularly in their proximal region. D genome chromosomes showed less divergence than the other genomes between “Kitahonami” and CS. Less SNP density in the 420-450 Mbp position of chromosome 2A and the short arm of chromosome 5D was uniquely detected in the mutant “30579.”

Large deletions are often observed in gamma-irradiated mutants [29, 30]. If a large deletion causes *Pina-D1* and *Pinb-D1* to be lost, a decrease of depth-of-coverage in the short arm of chromosome 5D should be uniquely observed in the mutant “30579.” To identify genomic regions where depth-of-coverage uniquely decreased in the mutant, we analyzed moving average of depth-of-coverage per three Mbp over the chromosomes (Fig. 3). Depth-of-coverage in the mutant was close to zero in 420-450 Mbp position of chromosome 2A, around 90 Mbp position of chromosome 4B, and 0-130 Mbp position of chromosome 5D, indicating that these chromosomal regions were uniquely deleted from “30579” mutant. The genome regions of the mutant “30579” showing less SNP density than the wild-type (Fig. 2) were consistent with these deleted regions. The distribution of difference of depth-of-coverage (Δdepth) per three Mbp between the wild-type and the mutant “30579” was also visualized over the chromosomes (Fig. 3). Peaks beyond the 99% confidence interval were observed at the uniquely deleted regions on chromosomes 2A, 4B, and 5B of the mutant “30579.” Several sharp peaks of Δdepth over 99% confidence interval corresponded to regions with irregularly deep depth-of-coverage, where mapped reads were derived from repetitive sequences. Since the chromosome 5D region with the large deletion corresponded to the genome region containing *Pina-D1* and *Pinb-D1* [12], the hard grain mutant “30579” lost *Pina-D1* and *Pinb-D1*.

Genotyping of the mapping population with indel markers confirmed causal regions of hard grains in mutant “30579”

We developed a F_2 (n = 72) population of a cross between the wild-type and the mutant “30579” to evaluate segregation of grain hardness. The SKCS analysis was conducted to examine grain hardness of the seeds harvested from the F_2 population. Of the tested lines, 22, 42, and eight lines showed soft, intermediate, and hard grain phenotypes, respectively (Fig. 4a). To validate which deletions were linked to the hard grain phenotypes, indel markers were designed for each deletion (Fig. 4b). Genotyping of 22 soft grain lines and eight hard grain lines was performed using the indel markers. The indel marker of chromosome 5D was linked to the hard grain phenotypes, whereas the indel markers of chromosomes 2A and 4B were not (Fig. 4c). This result indicates that the large deletion on chromosome 5D caused “Kitahonami” to change from soft to hard.

Characteristics of the PHS-tolerant mutant of “Kitahonami”

A PHS-tolerant mutant, called “28511,” was selected from “Kitahonami” mutant population. The PHS tolerance test showed that the mutant “28511” was more tolerant to PHS than the wild-type (Fig. 5, Table 3). PHS tolerance of the mutant “28511” was comparable to that of “Kitakei 1831,” used as a control variety for PHS tolerance. In the seed dormancy test, the mutant “28511” showed a lower germination rate than the wild-type under both 10 °C and 15 °C conditions in three seasons (Table 3). The mutant “28511” had higher germination rate than “Kitakei 1831” in 2016-2017 season whereas had similar germination rate to “Kitakei 1831” in 2017-2018 season. Agronomic and quality characteristics of the mutant “28511” were also evaluated (Table 4). Maturity stage, flour yield, and flour color of the mutant “28511” were almost the same as those of the wild-type. However, grain weight (kg/10a) and 1000-grain weight of the mutant “28511” were inferior to those of the wild-type. Moreover, the mutant “28511” showed higher flour protein content than those of the wild-type.

Table 3 The tests of PHS tolerance and seed dormancy of wild-type “Kitahonami” and the mutant 28511

Season	Name	PHS tolerance test	Seed dormancy test	
		PHS level	Germination rate (%)	
		(0 — 5)	15 °C	10 °C
2016/2017	Kitahonami WT	1.1	64.7	96
	28511	0.3	27.5	83.7
	Kitakei 1838	0	8	54
2017/2018	Kitahonami WT	0.4	83.7	82.4
	28511	0.1	20	45.8
	Kitakei 1838	0.1	18	48
2019/2020	Kitahonami WT	—	72.0	82.0
	28511	—	13.7	26.0

Table 4 Agronomic and quality characteristics of wild-type “Kitahonami” and the mutant “28511”

	Kitahonami WT	28511
Agronomic characteristics		
Maturity stage (date)[1]	25th July	26th July
Grain weight (kg/10a)	747	646
Ratio (%)	100	87
1000-grain weight (g)	41.5	36.9
Quality characteristics		
Grain protein content (%)	11.2	13.0
Flour ash content (%)	1.01	1.07
Flour yield (%)	71.0	70.1
Flour color L*	87.34	86.55
a*	-0.94	-0.56
b*	15.43	14.38

[1]Maturity stage was examined in 2016-2017 season.

Whole genome resequencing of the PHS-tolerant mutant “28511” identified a large deletion on the long arm of chromosome 3B

To identify the causal region of PHS tolerance of the mutant “28511,” genome sequencings of the mutant were performed in the same method as the hard grain mutant “30579.” Of the qualified 2.1 billion reads, 99.9% were successfully aligned to the reference genome of CS (Table 2). Average depth-of-coverage for the mutant was 19.43 for the mutant. The number of SNPs and short indels between the mutant “28511” and CS were 35,368,664 and 1,865,274, respectively. Uneven distribution of SNP density over chromosome for the mutant “28511” was also observed as shown in that of the wild-type and the mutant “30579” (Additional file 2: Fig. S1).

To detect deletions in the mutant “28511,” moving averages of depth-of-coverage per 3 Mbp and Δdepth per 3 Mbp were calculated over the chromosomes. At around 700 Mbp position of chromosome 3B, depth-of-coverage uniquely decreased in the mutant “28511” (Fig. 6). Δdepth also showed above 99% confidence interval. The reduced area extended to 67.8 Mbp, indicating that the mutant “28511” had a large deletion at the long arm of chromosome 3B. Such a remarkable reduction of depth-of-coverage was not observed in the other chromosomes.

Association between the large deletion at chromosome 3B and PHS tolerance

To validate the large deletion at chromosome 3B, we constructed a co-dominant marker to detect the deletion (Fig. 7a, Additional file 1: Table S1). Primer pairs (pre- and post-deletion primers) were designed outside the deletion boundary. Another primer (in-deletion primer) was designed inside the deletion boundary. In wild-type, a 712 bp PCR fragment amplified by in-deletion primer and post-deletion primer was observed, whereas in the mutant, a 414 bp PCR fragment amplified by pre-deletion primer and post-deletion primer was observed (Fig. 7b). When the CS nulli-tetrasomic line of nulli-3B tetra-3D, the chromosome 3B of which is replaced with chromosome 3D, was used, no PCR fragment was detected, indicating that this marker was specific to the deletion detected on chromosome 3B.

To confirm whether the large deletion was the causal genetic factor of PHS tolerance, we tested germination rate under the three conditions, three, seven, and nine days at 15 °C after seed sowing, for F_2 segregation population from a cross between the wild-type and the mutant “28511.” Also, we examined the genotype for the F_2 population by using the co-dominant marker, whether the large deletion was associated with low germination rate. Under every condition, the wild-type genotype had significantly high germination rate, followed by the heterozygous genotype, and the mutant genotype had the lowest germination rate (Fig. 7c). This result indicates that a large deletion was associated with the low germination rate, which could facilitate PHS tolerance of the mutant “28511.”

Since ABA sensitivity rather than the ABA level in seeds regulates seed dormancy, wheat plants with low ABA sensitivity decrease seed dormancy, resulting in PHS [31]. To test the ABA sensitivity of the wild-type and the mutant “28511,” suppression rate of germinated root elongation under exogenous ABA treatment was examined. No significant difference in the suppression between “Kitahonami” and the mutant “28511” was detected (Fig. 7d), implying that they have similar ABA sensitivity.

Vp-B1, associated with PHS tolerance [25, 26], was located in the long arm of chromosome 3B where the large deletion was detected in the mutant “28511.” A gene encoding GRAS family transcription factor was also found as a candidate gene of PHS tolerance in this region. Gibberellic acid (GA) promotes seed germination by inducing biosynthesis of α-amylase and protease in aleurone layers [32]. GRAS family transcription factor *SCARECROW-LIKE 3* (*SCL3*) is a positive regulator of GA signaling in *A. thaliana* [33]. We designed two markers for each gene to test whether these genes were lacking in the mutant (Fig. 8a). The markers for *Vp-B1* (Vp-1B_2 and Vp-1B_3) showed no amplification in the mutant “28511” and the nulli-3B tetra-3D line. The markers for GRAS family transcription factor (GRAS-TF_2 and GRAS-TF_3) exhibited no amplification in the either the mutant “28511” or the nulli-3B tetra-3D line (Fig. 8b). These results confirmed that *Vp-B1* and GRAS family transcription factor were deleted in the mutant “28511.”

Verification of detection ability in the gamma-irradiated wheat mutant with whole genome sequencing

To reduce resequencing cost, it is essential to know how much depth-of-coverage is necessary to detect large deletions in a gamma-irradiated mutant genome. By subsampling short reads and adjusting average depth-of-coverage per genome, we evaluated the deletion detection power of the method based on depth-of-coverage, visualized over chromosomes. Four depth-of-coverage conditions, 2.5x, 5x, 10x,

and 15x were tested using short reads from the PHS mutant “28511” and the wild-type (Fig. 9). The distributions of moving average of depth-of-coverage and Δdepth over the chromosomes were almost identical among all the conditions. The 67.8 Mbp deletion on chromosome 3B was significantly detected under all the depth-of-coverage conditions, implying that over 2.5x depth-of-coverage was enough to detect the large deletion in the gamma-irradiated wheat mutant.

In addition, to clarify how long deletions could be detected under the 5x depth-of-coverage conditions, simulation of deletion length was conducted by changing deletion length to 40 Mbp, 20 Mbp, 10 Mbp, 5 Mbp, 3 Mbp, and 1 Mbp (Fig. 10). When the deletion length was 1 Mbp or more, Δdepth was beyond 99% confidence interval. The length of the detectable deletion was found to depend on the window size of moving average. If window size was larger than the length of targeted deletion, the detectability of deletion decreased. For example, when the target deletion length was 3 Mbp, the estimated Δdepth for the 3 Mbp or 1 Mbp window size was over 99% confidence interval, but the estimated Δdepth for more than 3 Mbp window size was not. Another peak of Δdepth around 200 Mbp position on the chromosome. This detected peak was caused by repeats derived from transposable elements. By confirming both distributions of depth-of-coverage and Δdepth, such irregular peaks can be distinguished from deletions.

Characterization of mutations detected in the gamma-irradiated wheat mutants

Nucleotide substitutions and small indels with less than 25 bp, which was the maximum length detected by indel calling of bcftools, were also detected in the gamma-irradiated wheat mutants (Table 5, Additional file 1: Table S2). Between the wild-type and the grain hardness mutant “30579,” 2,412 SNPs and 329 small indels were detected. Between the wild-type and the PHS-tolerant mutant “28511,” 2,715 SNPs and 266 small indels were detected. Gamma irradiation is assumed to cause these SNPs and indels. The ratio of transition and transversion (Ts/Tv ratio) between the wild-type and the mutants is lower than that between the wild-type and CS and is regarded as a natural variation. Over 98% of SNPs were detected in the intergenic regions. SNPs between the wild-type and the mutants were more randomly distributed over chromosomes compared with SNP density between wild-type “Kitahonami” and CS (Fig. 2, Fig. 11, Additional file 2: Fig. S1). The limited natural variations on chromosomes 3A, 4A, 5A, 6A, 4B, 7B, and all the D genome chromosomes were observed between these two cultivars, while the putative mutations induced by gamma irradiation covered these chromosomes.

Table 5 Comparisons between putative gamma-irradiated and natural SNPs

	Wild-type vs. 30579 (Hard grain mutant)	Wild-type vs. 28511 (PHS tolerance mutant)	Wild-type vs. CS
Total	2,412	2,715	16,850,714
Transition	1,570 (65.091)	1,710 (62.983)	12,023,124 (71.351)
Transversion	842 (34.909)	1,005 (37.017)	4,827,590 (28.649)
Ts/Tv ratio	1.865	1.701	2.491
Exon	11 (0.455)	12 (0.442)	110,591 (0.651)
Synonymous	3 (0.124)	2 (0.074)	47,365 (0.279)
Nonsynonymous	8 (0.331)	10 (0.368)	63,226 (0.372)
Intron	15 (0.620)	20 (0.736)	252,919 (1.489)
UTRs	4 (0.165)	2 (0.074)	51,665 (0.304)
Intergenic	2,389 (98.760)	2,683 (98.749)	16,565,968 (97.555)
High impact variants[1]			
Total	0 (0.000)	1 (0.037)	1,696 (0.010)
Nonsense mutations	0 (0.000)	1 (0.037)	856 (0.005)
Start codon lost	0 (0.000)	0 (0.000)	93 (0.001)
Stop codon lost	0 (0.000)	0 (0.000)	282 (0.002)

Splice sites	0 (0.000)	0 (0.000)	465 (0.003)

Percentage is shown in parentheses.

[1]Variant types are defined in SnpEff (Cingolani et al. 2012).

Discussion

The usefulness of genome sequencing-based coverage analysis for deletions and duplications in the gamma-irradiated wheat mutants

The present study showed that genome sequencing-based coverage analyses of the gamma-irradiated wheat mutants could efficiently detect large deletions. Combined with segregation analyses in progeny population, deletions responsible for mutant phenotypes were successfully identified. The hard grain characteristic needs the expression of both PINA and PINB. The confirmation of the deletion of *Pina-D1* and *Pinb-D1* at the *Ha* locus in the grain hardness mutant “30579” demonstrates the usefulness of the comparative analysis of depth-of-coverage between wild-type and the mutant. In addition to the detection of large deletions, the analysis of depth-of-coverage allows detecting large duplications in gamma-irradiated wheat mutants. A putative large duplication was detected on the short arm of chromosome 1B in “30579” (Fig. 3). Depth-of-coverage is used as a parameter for detecting copy number variations [34] and segmental duplications [35]. The approach based on depth-of-coverage fits the detection of deletions and duplications in the gamma-irradiated wheat mutants.

The simulation results showed that short sequencing read data corresponding to 5x depth-of-coverage over genome was enough to detect five Mbp deletions visually. Furthermore, when Δdepth between wild-type and the mutant was used, even one Mbp deletion could be detected with over 95% confidential interval. The approach of Δdepth for the deletion detection is more powerful and provides evaluation criteria based on confidence interval. Detecting deletions in the gamma-irradiated mutants does not require high-coverage sequencing, reducing the cost of genome sequencing.

Characteristics of deletions and nucleotide mutations in the gamma-irradiated wheat mutants

The effectiveness of this approach could be unique to polyploid wheat with large genome. Double-stranded DNA breaks induced by gamma irradiation cause large deletions over one Mbp in plant [36, 37]. Inheritance of over one Mbp deletion to progeny is often impeded in *A. thaliana* and rice, which are diploid and have a relatively compact genome [29, 36]. The removal of genes involved in viability or gametogenesis is a potential factor in inhibiting the inheritance of large deletions, although the mechanisms have not yet been elucidated. On the other hand, whole genome sequencing of the gamma-irradiated wheat mutants identified the ~130 Mbp deletion at chromosome 5D and the 67.8 Mbp deletion at chromosome 3B. These large deletions were conservatively inherited to M_7 generations (See Methods). The continuous existence of large deletions over generations could be associated with polyploidy. The

hexaploid wheat has three homoeologous genes located on each of A, B, and D genomes. Even when one of the homoeologous genes are lost due to Mbp deletions, the other corresponding homoeologous genes can mitigate deleterious effects on viability. The aneuploid stocks are established in common wheat. The nullisomic lines, which lost one whole chromosome, are used for genetic research in wheat [38]. The deletion stocks of common wheat are also generated [39]. The large deletions in these stocks are stably inherited by the offspring. The large deletions above one Mbp generated by gamma irradiation are highly likely to be stably transmitted to the offspring due to compensation of the homoeologous chromosomes. It is speculated that two double-strand breaks followed by removal of the large fragment and subsequent re-ligation at two separated ends of the same chromosome produce a large deletion [36, 40]. Two double strand breaks could cause the large deletions inside the chromosomal ends in the tested gamma-irradiated mutants.

Genome sequencing of the gamma-irradiated wheat mutants also detected SNPs and small indels putatively induced by gamma irradiation. The random distribution of SNPs and small indels supports that the gamma irradiation induced these detected SNPs and indels (Fig. 11). In natural nucleotide variations, transition is more frequently observed than transversion due to differences in the ring structures of nucleobases and amino acid substitution frequency between transition and transversion, although transversion has twice as many nucleotide changes as transition. The Ts/Tv ratio of putative mutations introduced by gamma irradiation was lower than that of natural variations, although transition still occur more frequently than transversion (Table 5). Since mutations generated by gamma irradiation do not have evolutionary selective constraints on amino acid substitutions, the observed Ts/Tv ratio in the mutations generated by gamma irradiation could reflect only the differences in the ring structures of nucleobases. Given that the assembly size of the wheat reference genome is 14.5 Gbp [8] the number of SNP and indel per site are estimated to be ~2 x 10^{-7} and ~2 x 10^{-8}, respectively, although these values are potentially underestimated. Given that high impact SNPs and indels that potentially influence phenotypes were rare in the “Kitahonami” mutants (Table 5), structural variations such as large deletions and duplications could be the main cause of phenotypic changes in the gamma-irradiated mutants of hexaploid wheat.

The causative gene of the PHS tolerance of the “Kitahonami” mutant “28511”

Whole genome distribution of depth of coverage in the PHS tolerance mutant “28511” clarified the 67.8 Mbp large deletion at chromosome 3B (Fig. 6). The co-dominant marker designed for detecting the 67.8 Mbp deletion revealed a statistically significant association between this deletion and PHS tolerance in the F_2 segregating population (Fig. 7c). Two PHS-related genes, GRAS family transcription factor (TraesCS3B01G441600) and *Vp-1*, are located in the deleted region. The deletion of these genes was confirmed by no PCR amplification of these genes from genomic DNA of the PHS-tolerant mutant.

GRAS family has the highly conserved C-terminal GRAS domain. *A. thaliana* has 33 genes encoding GRAS family transcription factor, which includes DELLA protein family involved in GA signaling in plants [33, 41, 42]. *Rht-B1*, which causes semi-dwarfism in wheat and led to the wheat green revolution, also

belong to GRAS family [43]. TraesCS3B01G441600 is close to *AtSCL1* and *AtPAT1* and is separated from *Rht-B1* and the gene encoding the positive regulator of GA signaling, *AtSCL3* [33] (Additional file 2: Fig. S2). TraesCS3B01G441600 can be classified into *AtPAT1* subfamily [44]. *AtPAT1* is involved in phytochrome light signaling rather than GA signaling. *OsCIGR1* and *OsCIGR2*, rice GRAS family transcription factors belonging to *AtPAT1* subfamily, are induced by exogenous GA in rice suspension culture but cannot be involved in mechanisms of α-amylase expression in aleurone layer [45]. Considering the function of genetically close homologs in *A. thaliana* and rice, TraesCS3B01G441600 is unlikely to be the causative gene of the PHS-tolerant mutant.

The *Vp-1* positively contributes to seed maturation, dormancy, and ABA sensitivity in maize, *A. thaliana* and wheat [25, 46, 47, 48], repressing germination. The loss of function of *Vp-1* in maize and *ABI3*, the homolog of *Vp-1*, in *A. thaliana* arrests embryo maturation and decreases ABA sensitivity, resulting in precocious germination [46, 47, 48]. The “Kitahonami” mutant “28511” lost *Vp-1* gene on chromosome 3B but increased PHS tolerance. In addition, the “Kitahonami” mutant “28511” did not reduce ABA sensitivity. These observations contradict those in diploid plants, maize, and *A. thaliana*. Given that hexaploid wheat has three homoeologous genes of *Vp-A1*, *Vp-B1*, and *Vp-D1*, encoding full-length protein [49], VP-A1 and VP-D1, could compensate for the VP-B1 function, preventing the reduction of ABA sensitivity and blocking precocious germination. To confirm this hypothesis, further experiments are needed.

Conclusion

In this study, we selected the grain hardness mutant “30579” and the PHS-tolerant mutant “28511” form gamma-irradiated mutants of Japanese elite cultivar “Kitahonami” and performed whole-genome resequencing of these mutant lines. The comparative analysis of depth-of-coverage between the wild-type and the mutants identified ~130 Mbp and 67.8 Mbp deletions in the mutants “30579” and “28511,” respectively. These deletions were tightly linked to the mutant phenotypes in the progeny populations generated by crosses between wild-type and the mutants. The simulation analyses showed that 2.5x depth-of-coverage was enough to detect large deletions in the gamma-irradiated hexaploid wheat mutants. These results indicate that the approach of short-read-based genome sequencings of the gamma-irradiated mutants is cost-effective in designing genetic markers for agriculturally beneficial traits to breeding of wheat.

Abbreviations

PHS: pre-harvest sprouting

HA: hardness

SKCS: single kernel characterization system

ABA: abscisic acid

Declarations

We comply with the IUCN Policy Statement on Research Involving Species at Risk of Extinction and the Convention on the Trade in Endangered Species of Wild Fauna and Flora.

Ethics approval and consent to participate

Not applicable

Consent for publication

Not applicable

Availability of data and materials

The genome sequencing data generated during the current study are available in the database of the Komugi GSP (Genome Sequencing Program) (https://komugigsp.dna.affrc.go.jp/research/download/index.html). The R and python scripts used in this study are available from the GitHub repository (https://github.com/ShoyaKomura/WheatGammaIrradiationMutGenomeSeq). The plant materials used and/or analyzed during the current study are available from the corresponding author on reasonable request.

Competing interests

The authors declare that they have no competing interests. The research was conducted in the absence of any commercial or financial relationships that could be construed as a potential conflict of interest.

Funding

KY, ST, HJ, TS, and FK are supported by a grant from the Ministry of Agriculture, Forestry and Fisheries of Japan [Smart-breeding system for Innovative Agriculture (DIT1002)]. HJ, TS, YO, HH, and FK are supported a grant from the Ministry of Agriculture, Forestry and Fisheries of Japan [Genomics-based Technology for Agricultural Improvement (IVG1003)].

Authors' contributions

HJ, TS, YO, HH, and FK generated gamma-irradiated mutants and selected the PHS and hard grain mutants. HJ, TS, FK, and SK evaluated phenotypes of the mutants. SK and KY analyzed genome sequencing data. YO, HH, and FK generated and analyzed wild-type "Kitahonami" genome sequencing data. SK performed genotyping. HJ, FK, ST, and KY designed experiments and genome sequencing analyses. SK, KY, and FK wrote the manuscript.

Acknowledgements

Computations were partially performed on the NIG supercomputer at ROIS National Institute of Genetics, Japan. Chinese Spring nulli-tetrasomic lines were provided by the National BioResource Project-Wheat with support in part by National BioResource Project of the MEXT, Japan

References

1. Shu QY, Forster BP, Nakagawa H. eds. Plant mutation breeding and biotechnology. Cambridge, MA: CABI; 2012.
2. Holme IB, Gregersen PL, Brinch-Pedersen H. Induced genetic variation in crop plants by random or targeted mutagenesis: Convergence and Differences. Front Plant Sci. 2019;10:1–9.
3. Singh B, Datta PS. Gamma irradiation to improve plant vigour, grain development, and yield attributes of wheat. Radiat Phys Chem. 2010;79:139–43. doi:10.1016/j.radphyschem.2009.05.025.45.
4. Hossain KG, Riera-Lizarazu O, Kalavacharla V, Vales MI, Maan SS, Kianian SF. Radiation hybrid mapping of the species cytoplasm-specific (scs ae) gene in wheat. Genetics. 2004;168:415–23.
5. Kumar A, Seetan R, Mergoum M, Tiwari VK, Iqbal MJ, Wang Y, et al. Radiation hybrid maps of the D-genome of *Aegilops tauschii* and their application in sequence assembly of large and complex plant genomes. BMC Genomics. 2015;16:1–14.
6. Cheng X, Chai L, Chen Z, Xu L, Zhai H, Zhao A, et al. Identification and characterization of a high kernel weight mutant induced by gamma radiation in wheat (Triticum aestivum L.). BMC Genet. 2015;16:1–9.
7. Jia S, Li A, Morton K, Avoles-Kianian P, Kianian SF, Zhang C, et al. A population of deletion mutants and an integrated mapping and exome-seq pipeline for gene discovery in maize. G3 Genes, Genomes, Genet. 2016;6:2385–95.
8. International Wheat Genome Sequencing Consortium (IWGSC). Shifting the limits in wheat research and breeding using a fully annotated reference genome. Science 2018;361:eaar7191.
9. Walkowiak S, Gao L, Monat C, Haberer G, Kassa MT, Brinton J, et al. Multiple wheat genomes reveal global variation in modern breeding. Nature. 2020;588:277–83.
10. Zhou Y, Zhao X, Li Y, Xu J, Bi A, Kang L, et al. Triticum population sequencing provides insights into wheat adaptation. Nat Genet. 2020;52:1412–22.
11. Wheat breeding group of Kitami Agricultural Experiment Station, Hokkaido Research Organization. Breeding of a high yielding and pre-harvest sprouting tolerant winter wheat variety “Kitahonami” with superior processing qualities for Hokkaido. Breed Res. 2015;17:134–8.
12. Sourdille P, Perretant MR, Charmet G, Leroy P, Gautier MF, Joudrier P, et al. Linkage between RFLP markers and genes affecting kernel hardness in wheat. Theor Appl Genet. 1996;93:580–6.46.
13. Giroux MJ, Morris CF. Wheat grain hardness results from highly conserved mutations in the friabilin components puroindoline a and b. Proc Natl Acad Sci U S A. 1998;95:6262–6.

14. Morris CF. Puroindolines: the molecular basis of wheat grain hardness. Plant Mol Biol. 2015;48:633–47.
15. Gasparis S, Orczyk W, Zalewski W, Nadolska-Orczyk A. The RNA-mediated silencing of one of the Pin genes in allohexaploid wheat simultaneously decreases the expression of the other, and increases grain hardness. J Exp Bot. 2011;62:4025–36.
16. Gasparis S, Kała M, Przyborowski M, Orczyk W, Nadolska-Orczyk A. Artificial microRNA-based specific gene silencing of grain hardness genes in polyploid cereals appeared to be not stable over transgenic plant generations. Front Plant Sci. 2017;7:1–13.
17. Kottearachchi NS, Uchino N, Kato K, Miura H. Increased grain dormancy in white-grained wheat by introgression of preharvest sprouting tolerance QTLs. Euphytica. 2006;152:421–8.
18. Mohan A, Kulwal P, Singh R, Kumar V, Mir RR, Kumar J, et al. Genome-wide QTL analysis for pre-harvest sprouting tolerance in bread wheat. Euphytica. 2009;168:319–29.
19. Nakamura S. Grain dormancy genes responsible for preventing pre-harvest sprouting in barley and wheat. Breed Sci. 2018;68:295–304.37.
20. Olaerts H, Courtin CM. Impact of Preharvest Sprouting on Endogenous Hydrolases and Technological Quality of Wheat and Bread: A Review. Compr Rev Food Sci Food Saf. 2018;17:698–713.39.
21. Chono M, Matsunaka H, Seki M, Fujita M, Kiribuchi-Otobe C, Oda S, et al. Molecular and genealogical analysis of grain dormancy in japanese wheat varieties, with specific focus on mother of ft and tfl1 on chromosome 3a. Breed Sci. 2015;65:103–9.
22. Rasheed A, Takumi S, Hassan MA, Imtiaz M, Ali M, Morgunov AI, et al. Appraisal of wheat genomics for gene discovery and breeding applications: a special emphasis on advances in Asia. Theor Appl Genet. 2020;133:1503–20.
23. Nakamura S, Abe F, Kawahigashi H, Nakazono K, Tagiri A, Matsumoto T, et al. A wheat homolog of MOTHER of FT and TFL1 acts in the regulation of germination. Plant Cell. 2011;23:3215–3129.38.
24. Torada A, Koike M, Ogawa T, Takenouchi Y, Tadamura K, Wu J, et al. A causal gene for seed dormancy on wheat chromosome 4A encodes a MAP kinase kinase. Curr Biol. 2016;26:782–7.
25. Nakamura S, Toyama T. Isolation of a VP1 homologue from wheat and analysis of its expression in embryos of dormant and non-dormant cultivars. J Exp Bot. 2001;52:875–6.36.
26. Yang Y, Ma YZ, Xu ZS, Chen XM, He ZH, Yu Z, et al. Isolation and characterization of Viviparous-1 genes in wheat cultivars with distinct ABA sensitivity and pre-harvest sprouting tolerance. J Exp Bot. 2007;58:2863–71.54.
27. Abe F, Haque E, Hisano H, Tanaka T, Kamiya Y, Mikami M, et al. Genome-Edited Triple-Recessive Mutation Alters Seed Dormancy in Wheat. Cell Rep. 2019;28:1362–1369.e4.
28. Himi E, Maekawa M, Miura H, Noda K. Development of PCR markers for Tamyb10 related to R-1, red grain color gene in wheat. Theor Appl Genet. 2011;122:1561–76.
29. Morita R, Kusaba M, Iida S, Yamaguchi H, Nishio T, Nishimura M. Molecular characterization of mutations induced by gamma irradiation in rice. Genes Genet Syst. 2009;84:361–70.

30. Shirasawa K, Hirakawa H, Nunome T, Tabata S, Isobe S. Genome-wide survey of artificial mutations induced by ethyl methanesulfonate and gamma rays in tomato. Plant Biotechnol J. 2016;14:51–60.44.
31. Walker-Simmons M. ABA levels and sensitivity in developing wheat embryos of sprouting resistant and susceptible cultivars. Plant Physiol. 1987;84:61–6.51.
32. Gómez-Cadenas A, Zentella R, Walker-Simmons MK, Ho THD. Gibberellin/abscisic acid antagonism in barley aleurone cells: Site of action of the protein kinase PKABA1 in relation to gibberellin signaling molecules. Plant Cell. 2001;13:667–79.
33. Zhang ZL, Ogawa M, Fleet CM, Zentella R, Hu J, Heo JO, et al. SCARECROW-LIKE 3 promotes gibberellin signaling by antagonizing master growth repressor DELLA in Arabidopsis. Proc Natl Acad Sci U S A. 2011;108:2160–5.55.
34. Yoon S, Xuan Z, Makarov V, Ye K, Sebat J. Sensitive and accurate detection of copy number variants using read depth of coverage. Genome Res. 2009;19:1586–92.
35. She X, Cheng Z, Zöllner S, Church DM, Eichler EE. Mouse segmental duplication and copy number variation. Nat. Genet. 2008;40:909–14.
36. Naito K, Kusaba M, Shikazono N, Takano T, Tanaka A, Tanisaka T, et al. Transmissible and nontransmissible mutations induced by irradiating Arabidopsis thaliana pollen with γ-rays and carbon ions. Genetics. 2005;169:881–9.
37. Datta S, Jankowicz-Cieslak J, Nielen S, Ingelbrecht I, Till BJ. Induction and recovery of copy number variation in banana through gamma irradiation and low-coverage whole-genome sequencing. Plant Biotechnol J. 2018;16:1644–53.
38. Sears ER. The aneuploids of common wheat. Missouri Agr Expt Sta Res Bull. 1954;572:1–58.43.
39. Endo TR, Gill BS. The deletion stocks of common wheat. J Hered. 1996;87:295–307.
40. Sachs RK, Hlatkys LR, Trask BJ. Radiation-produced chromosome aberrations colourful clues Ionizing radiation produces many chromosome aberrations. A rich variety of aberration types can now be seen. 2000;16:143–6.42.
41. Bolle C. The role of GRAS proteins in plant signal transduction and development. Planta. 2004;218:683–92.
42. Hirsch S, Oldroyd GED. GRAS-domain transcription factors that regulate plant development. Plant Signal Behav. 2009;4:698–700.
43. Pearce S, Saville R, Vaughan SP, Chandler PM, Wilhelm EP, Sparks CA, et al. Molecular characterization of Rht-1 dwarfing genes in hexaploid wheat. Plant Physiol. 2011;157:1820–31.
44. Sun X, Xue B, Jones WT, Rikkerink E, Dunker AK, Uversky VN. A functionally required unfoldome from the plant kingdom: Intrinsically disordered N-terminal domains of GRAS proteins are involved in molecular recognition during plant development. Plant Mol Biol. 2011;77:205–23.47.
45. Day RB, Shibuya N, Minami E. Identification and characterization of two new members of the GRAS gene family in rice responsive to N-acetylchitooligosaccharide elicitor. Biochim Biophys Acta - Gene

Struct Expr. 2003;1625:261–8.

46. McCarty DR, Carson CB, Stinard PS, Robertson DS. Molecular Analysis of viviparous-1: An Abscisic Acid-Insensitive Mutant of Maize. Plant Cell. 1989;1:523.
47. McCarty DR, Hattori T, Carson CB, Vasil V, Lazar M, Vasil IK. The Viviparous-1 developmental gene of maize encodes a novel transcriptional activator. Cell. 1991;66:895–905.
48. Giraudat J, Hauge BM, Valon C, Smalle J, Parcy F, Goodman HM. Isolation of the Arabidopsis ABI3 gene by positional cloning. Plant Cell. 1992;4:1251–61.
49. McKibbin RS, Wilkinson MD, Bailey PC, Flintham JE, Andrew LM, Lazzeri PA, et al. Transcripts of Vp-1 homeologues are misspliced in modern wheat and ancestral species. Proc Natl Acad Sci U S A. 2002;99:10203–8.
50. Iehisa JCM, Shimizu A, Sato K, Nishijima R, Sakaguchi K, Matsuda R, et al. Genome-wide marker development for the wheat D genome based on single nucleotide polymorphisms identified from transcripts in the wild wheat progenitor Aegilops tauschii. Theor Appl Genet. 2014;127:261–71.
51. Andrews S. FastQC: a quality control tool for high throughput sequence data. 2010. http://www.bioinformatics.babraham.ac.uk/projects/fastqc. Accessed 7 Mar 2021.
52. Bolger AM, Lohse M., Usadel B. Trimmomatic: A flexible trimmer for Illumina sequence data. Bioinformatics. 2014;30:2114–20.
53. Li H, Durbin R. Fast and accurate short read alignment with Burrows-Wheeler transform. Bioinformatics. 2009;25:1754–60.
54. Li, H., Handsaker, B., Wysoker, A., Fennell, T., Ruan, J., Homer, N., et al. The Sequence Alignment/Map format and SAMtools. Bioinformatics. 2009;25:2078–2079. Doi:10.1093/bioinformatics/btp352.
55. Bushnell, BBMap: A Fast, Accurate, Splice-Aware Aligner. Berkeley, CA: Ernest Orlando Lawrence Berkeley National Laboratory; 2014.
56. Li H. A statistical framework for SNP calling, mutation discovery, association mapping and population genetical parameter estimation from sequencing data. Bioinformatics. 2011;27:2987–93.
57. Cingolani P, Platts A, Wang le L, Coon M, Nguyen T, Wang L, Land SJ, Lu X, Ruden DM. A program for annotating and predicting the effects of single nucleotide polymorphisms, SnpEff: SNPs in the genome of Drosophila melanogaster strain w1118; iso-2; iso-3. Fly (Austin). 2012;6:80–92.
58. Li H. seqtk: toolkit for processing sequences in FASTA/Q formats. https://github.com/lh3/seqtk. Accessed 1 Feb 2020.
59. Miki Y, Ikeda M, Yoshida K, Takumi S. Identification of a hard kernel texture line of synthetic allohexaploid wheat reducing the puroindoline accumulation on the D genome from *Aegilops tauschii*. J. Cereal Sci. 2020;93:102964.

Figures

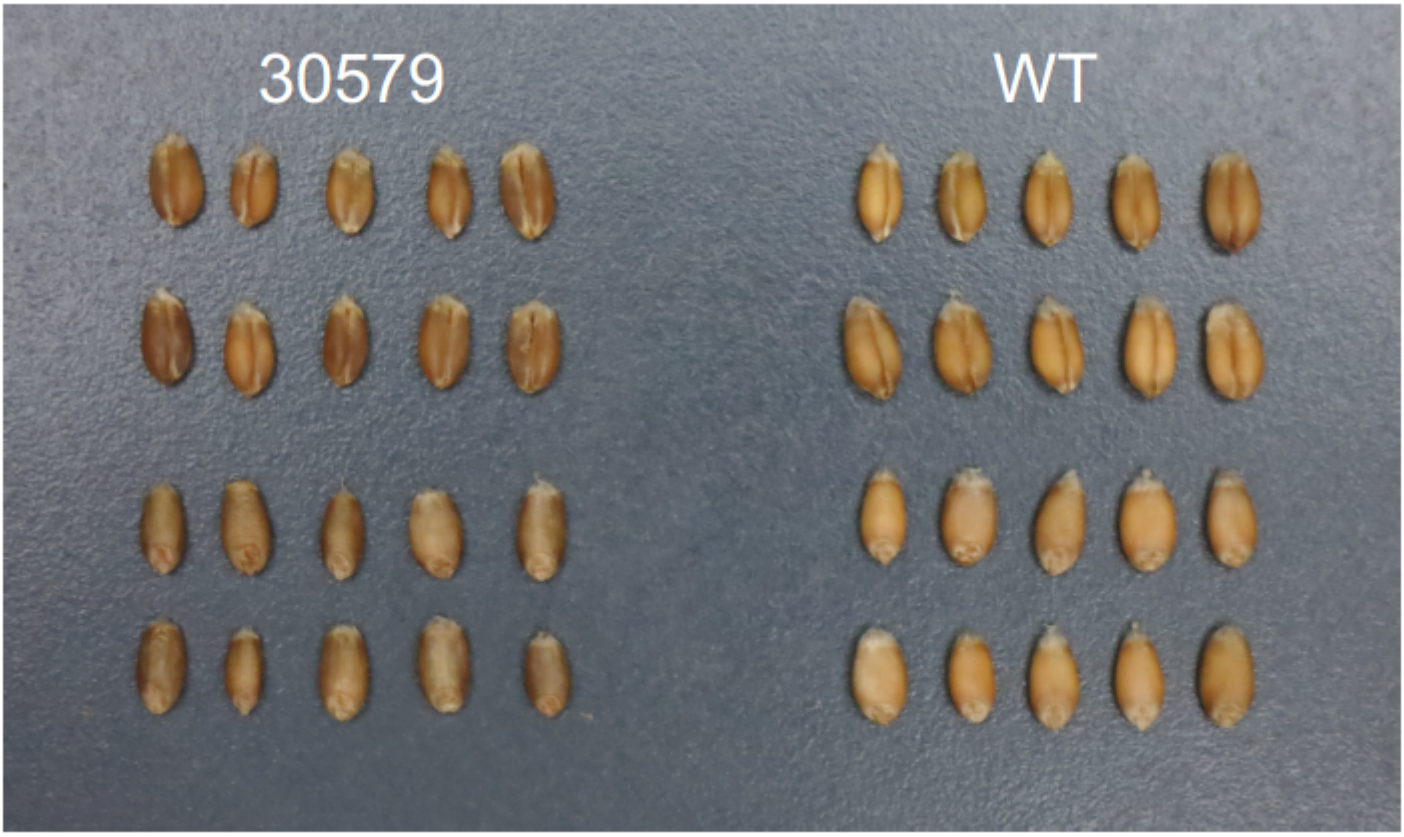

Figure 1

Morphology of the grain hardness mutant “30579” Grains of the mutant “30579” (left) and wild-type “Kitahonami” (right).

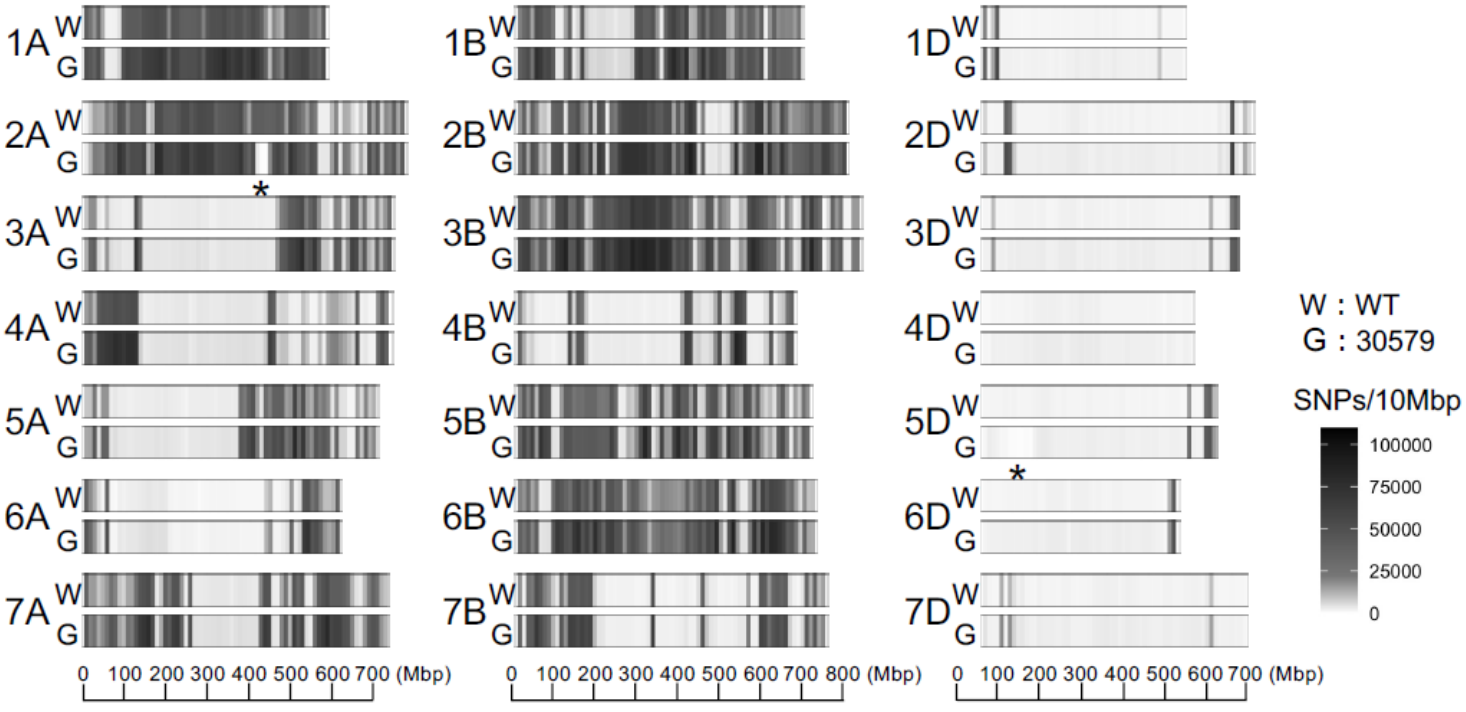

Figure 2

Distribution of SNPs between wheat cultivars “Kitahonami” and “Chinese Spring” or between the grain hardness mutant “30579” and “Chinese Spring” over the chromosomes. SNP density was estimated by counting number of SNPs per 10 Mbp. SNP density is displayed as the gradation color from white to black. The higher the density, the blacker it is. In the regions with an asterisk, the mutant shows less SNP density compared with the wild-type.

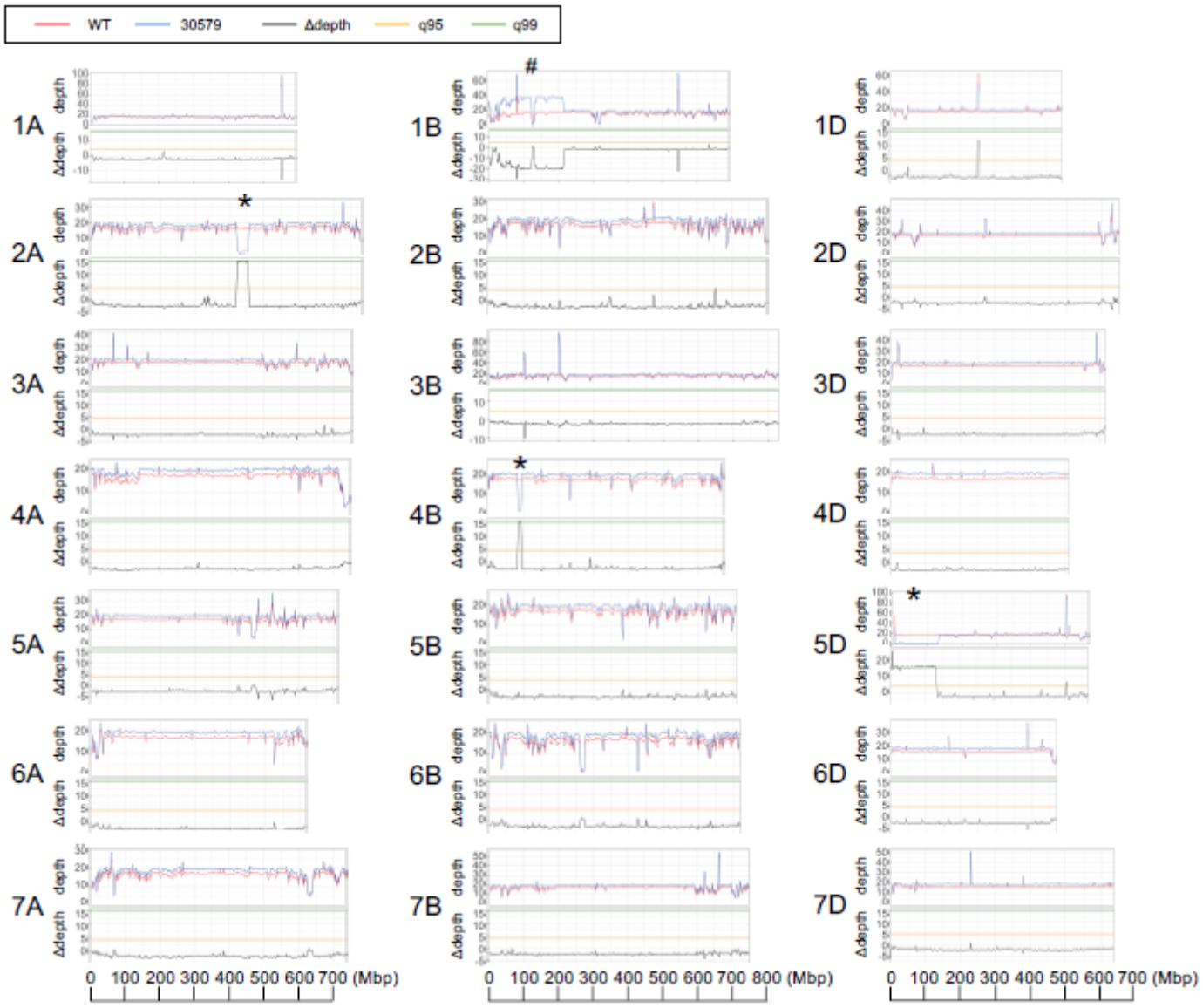

Figure 3

Depth of coverage of wild-type “Kitahonami” and the grain hardness mutant “30579” over chromosomes Distribution of moving average of depth-of-coverage and difference of depth-of-coverage (Δdepth) between wild-type “Kitahonami” and the mutant “30579” was visualized over chromosomes. q95 and q99 indicate 95% and 99% confidence intervals, respectively. Window size is 3 Mbp, and step size is 1 Mbp. An asterisk indicates a region with a large deletion. # indicates a large duplication.

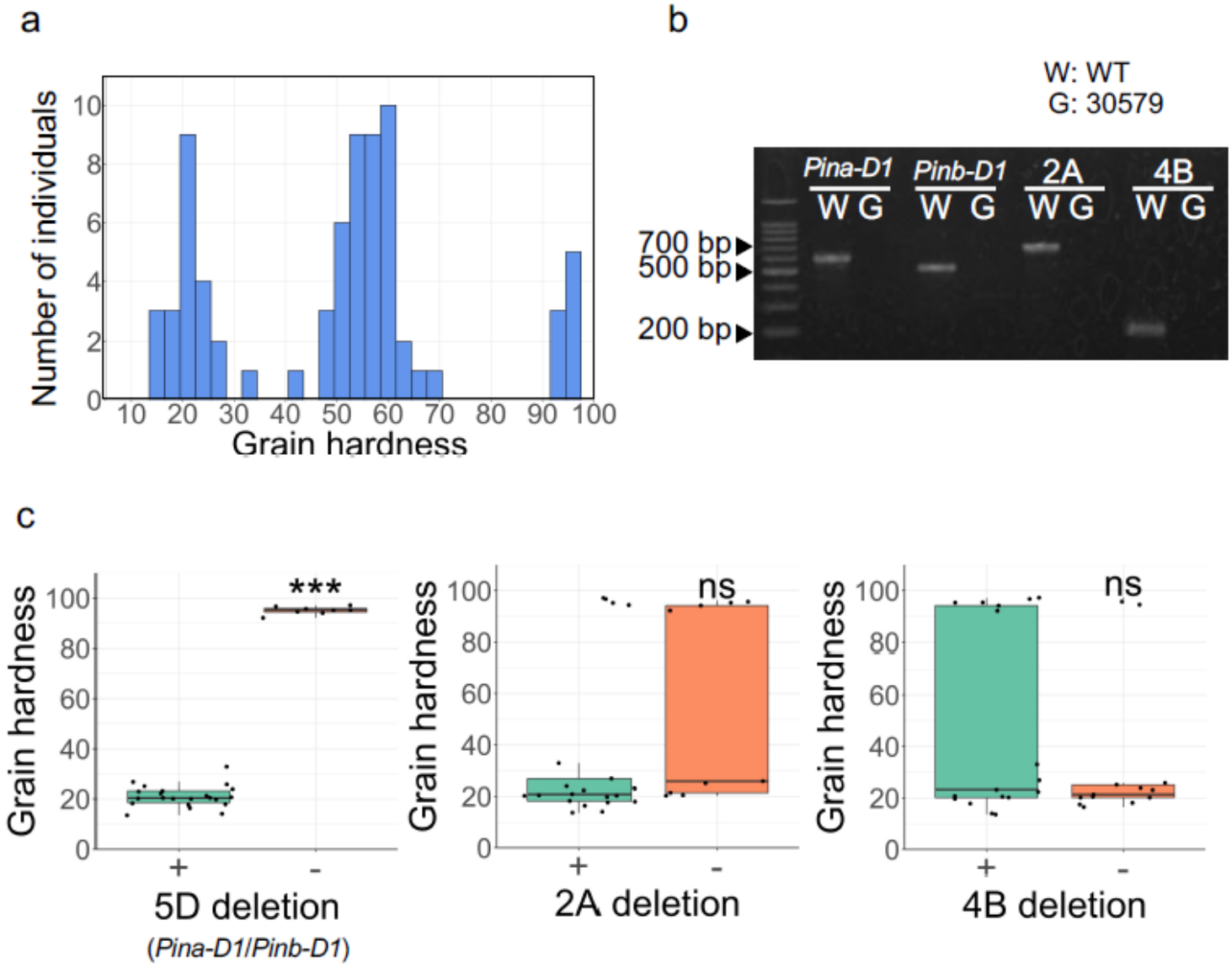

Figure 4

Grain hardness of F2 individuals of the cross between wild-type “Kitahonami” and the grain hardness mutant “30579” (a) The histogram of grain hardness of F2 individuals. (b) The results of PCR amplification of the indel markers of 5D (Pina-D1 and Pinb-D1), 2A, and 4B. W and G indicate the wild-type and the mutant, respectively. (c) Relationship between grain hardness and genotypes in 5D, 2A, and 4B deletions. Boxplots of grain hardness and genotypes of each deletion are shown. Dots in the boxplots indicate grain hardness for each sample. Genotypes of 22 soft grain and eight hard grain lines were evaluated based on the indel markers for 5D (Pina-D1 and Pinb-D1), 2A, 4B deletions. + indicates absence of deletion, and – indicates presence of deletion. Students’ t-test was performed to test statistically significant differences between genotypes. ***P < 0.01, ns: non-significant.

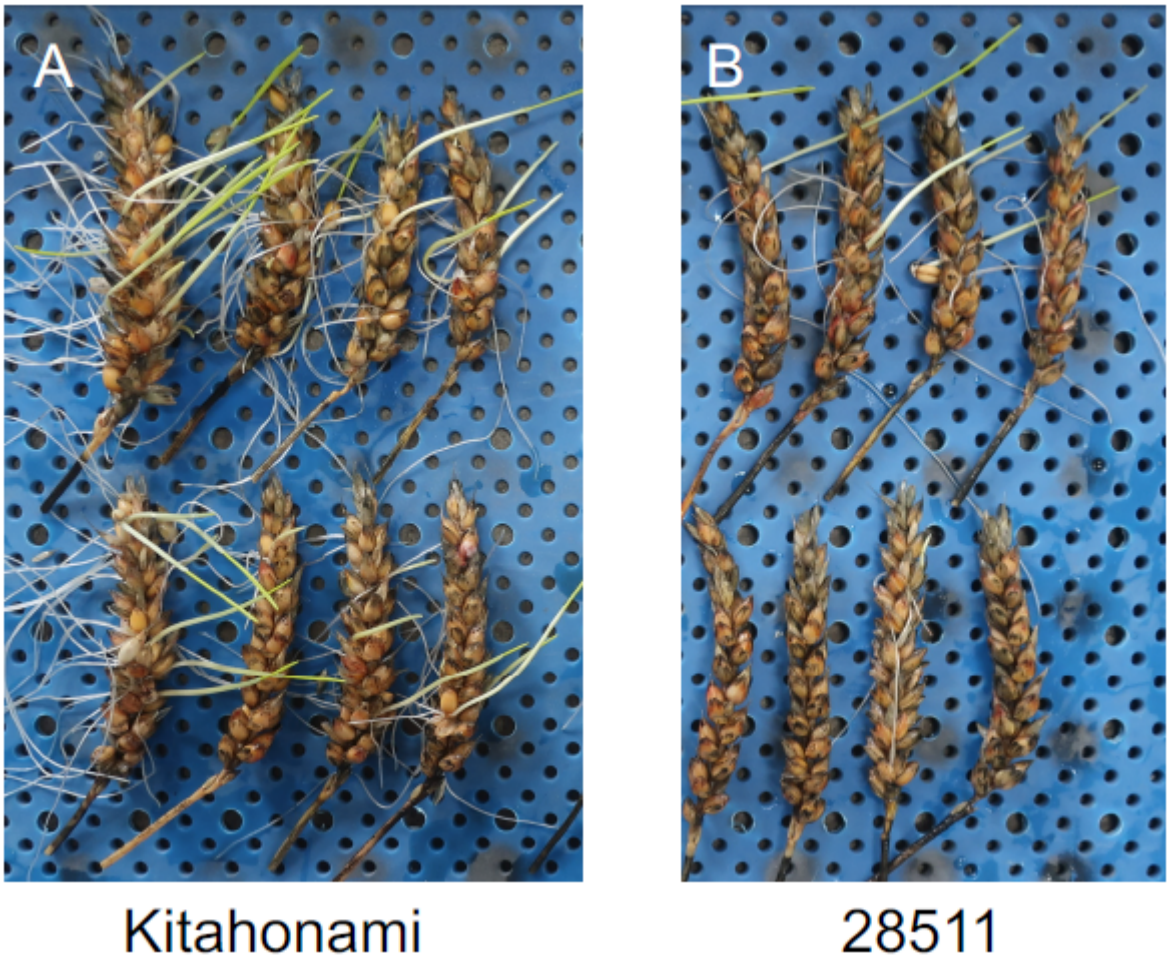

Figure 5

Pre-harvest sprouting tolerance of “Kitahonami” mutant “28511” Eight spikes of wild-type “Kitahonami” (A) and the mutant “28511” (B) are shown.

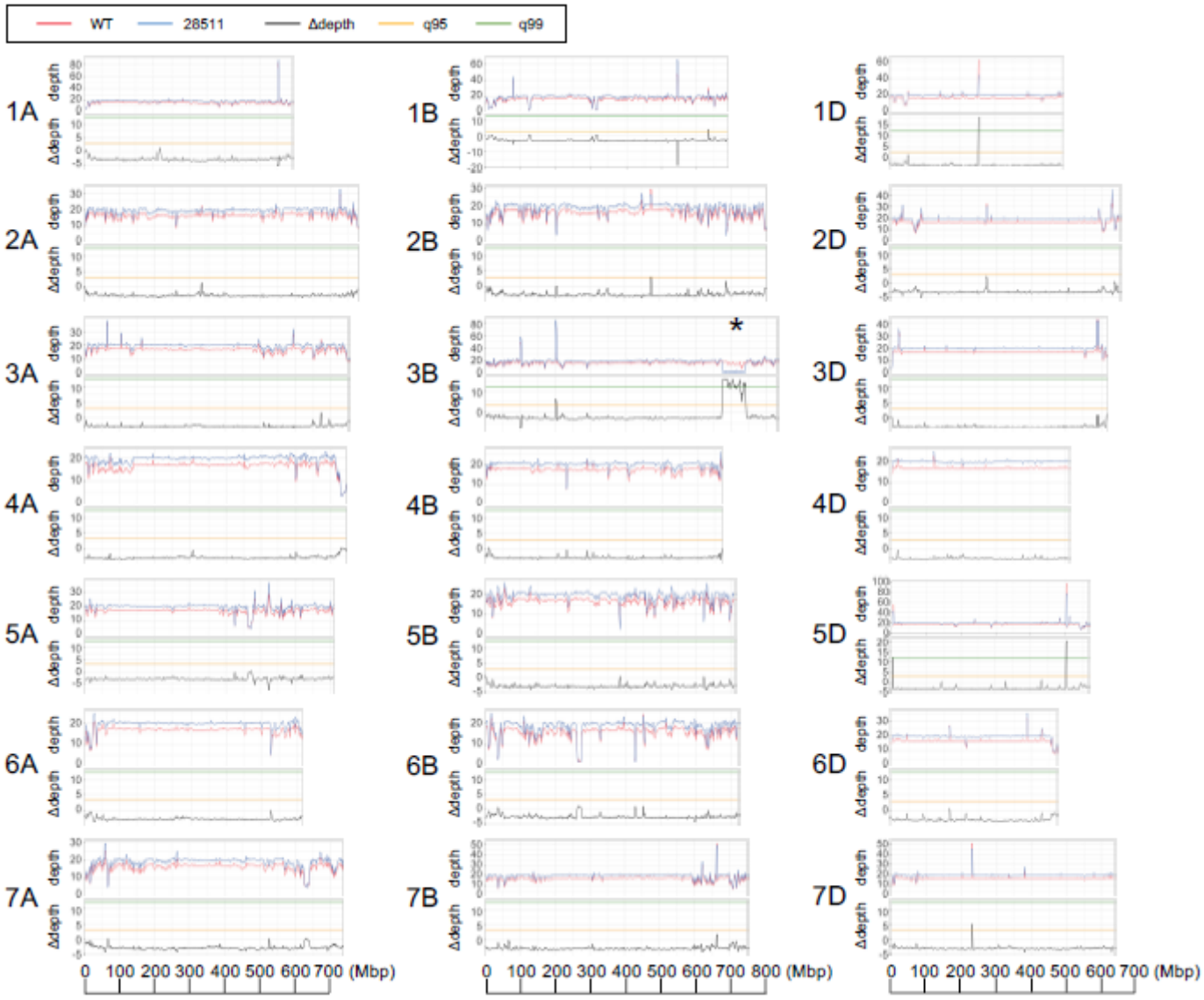

Figure 6

Depth of coverage of wild-type “Kitahonami” and the pre-harvest sprouting mutant “28511” over chromosomes Distribution of moving average of depth-of-coverage and difference of depth-of-coverage (Δdepth) between wild-type “Kitahonami” and the mutant “28511” was visualized over chromosomes. q95 and q99 indicate 95% and 99% confidence intervals, respectively. Window size is 3 Mbp, and step size is 1 Mbp. An asterisk indicates a region with a large deletion.

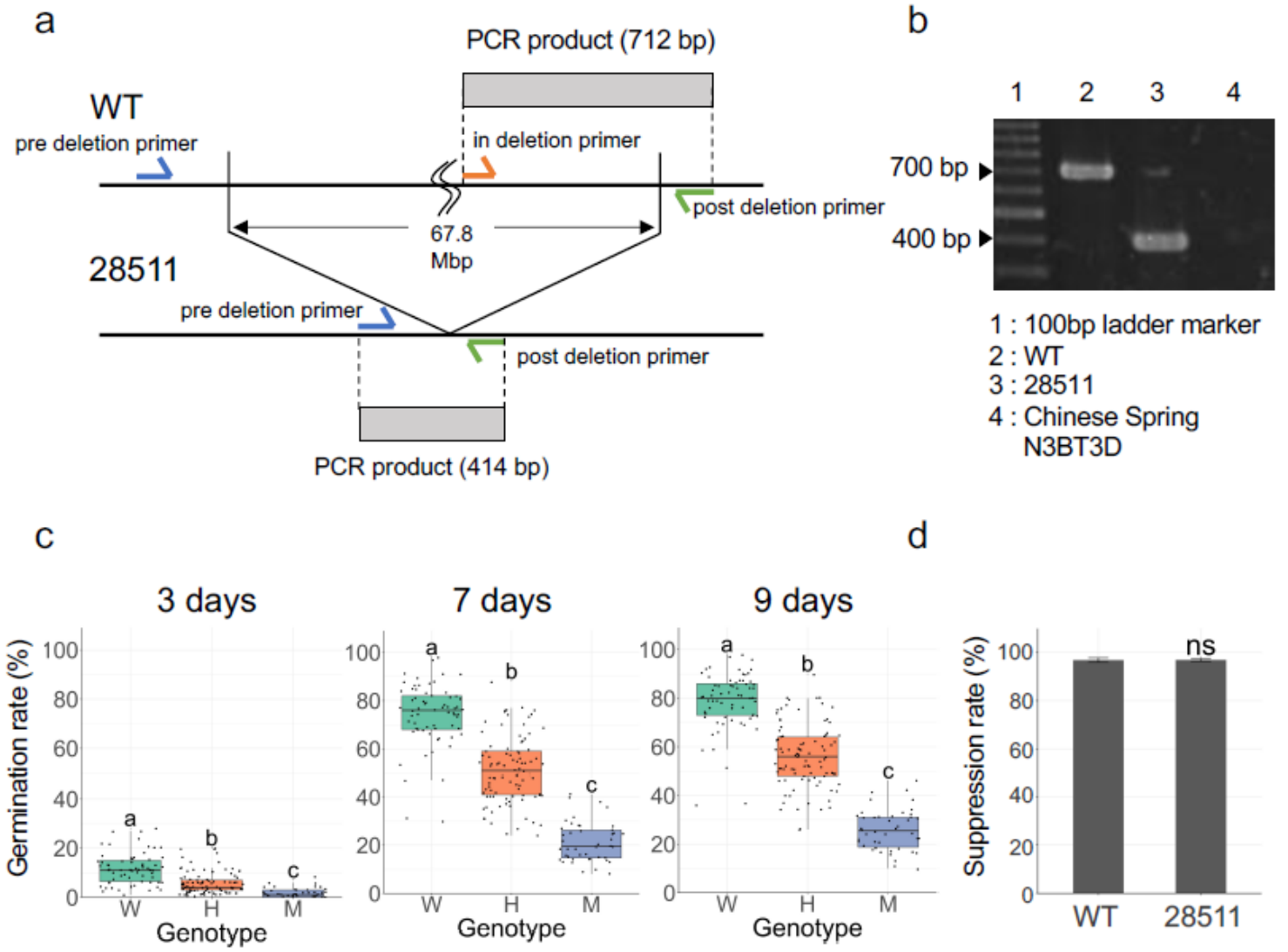

Figure 7

Associations between PHS tolerance and the deletion on chromosome 5D in the F2 population (a) A diagram of co-dominant markers to detect the deletion on chromosome 5D. A 712 bp PCR fragment is amplified by “in deletion” primer and “post deletion” primer is expected in wild-type Kitahonami (WT). A 414 bp PCR fragment is amplified by “pre deletion” primer and “post deletion” primer in the PHS tolerance mutant 28511. Both of these fragments are amplified in heterozygous individuals in F2 population. (b) Results of PCR amplification of co-dominant markers in WT, 28511, and the Chinese Spring nulli-tetrasomic line N3BT3D in which chromosome 3B is replaced with chromosome 3D. (c) The seed dormancy test for the F2 segregation population of Kitahonami WT X the mutant 28511. Boxplots of germination rate for each genotype in 3 days, 7 days, and 9 days are shown. The dots indicate germination rate for each sample. W, H, and M are homozygous alleles of WT, heterozygous alleles of WT and the mutant, homozygous alleles of the mutant, respectively. (d) The ABA sensitivity test in WT and the mutant. ns: not significant in student’s t-test.

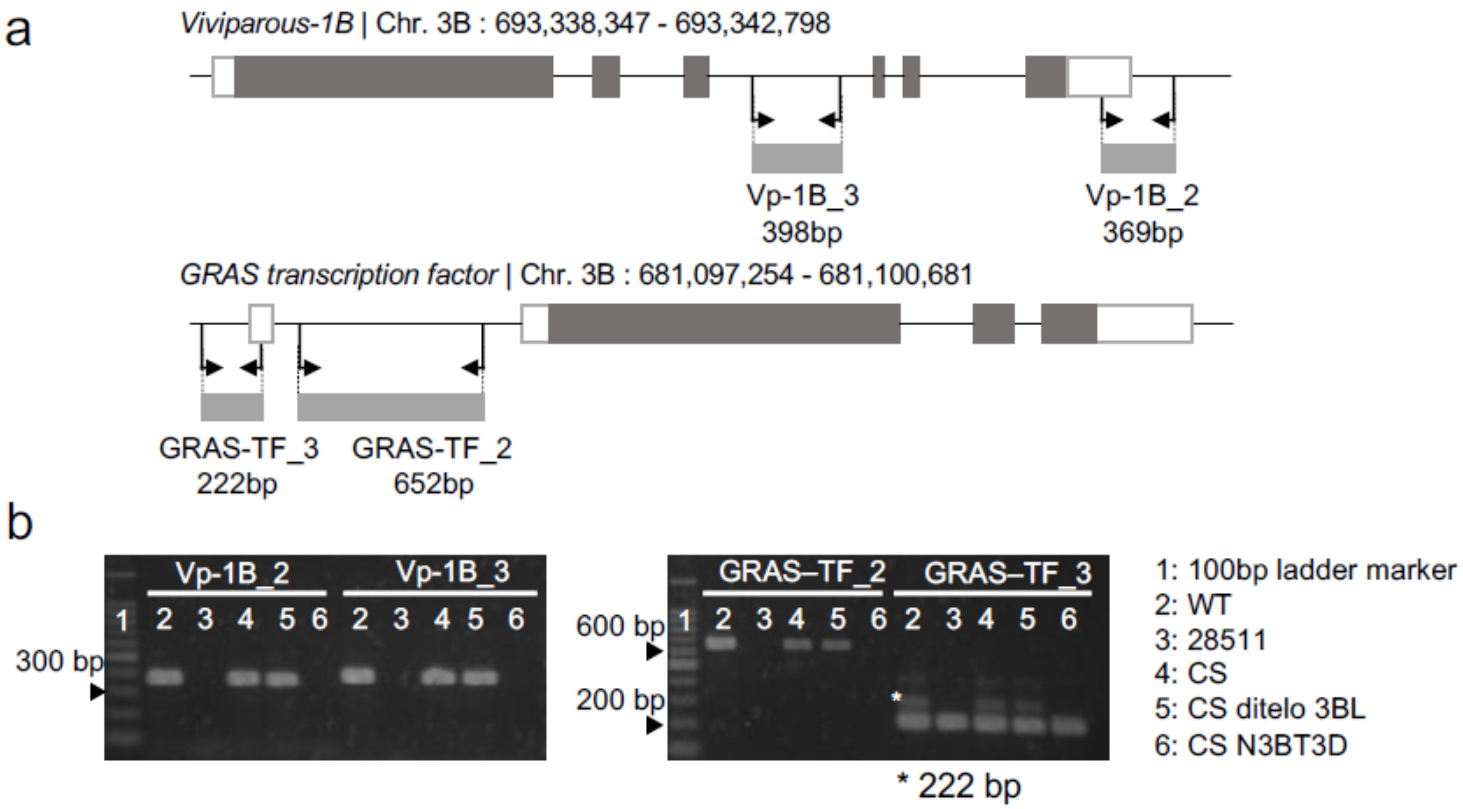

Figure 8

Relationship between PHS tolerance and presence/absence of the candidate genes on chromosome 3D. (a) Primer positions of Viviparous-B1 and the GRAS transcription factor gene to confirm presence/absence of these genes in “Chinese Spring” (CS) deletion lines at chromosome 3B (Endo and Gill, 1996). (b) The two primer sets were designed to amplify two fragments for each gene. PCR amplifications of Viviparous-1B and the GRAS transcription factor gene in wild-type “Kitahonami” (WT), the PHS-tolerant mutant “28511”, CS, the CS 3BL ditelosomic line (CS ditelo 3BL), and the CS nulli-tetrasomic line of nulli-3B tetra-3D (CS N3BT3D). Three independent tests of seed dormancy were conducted.

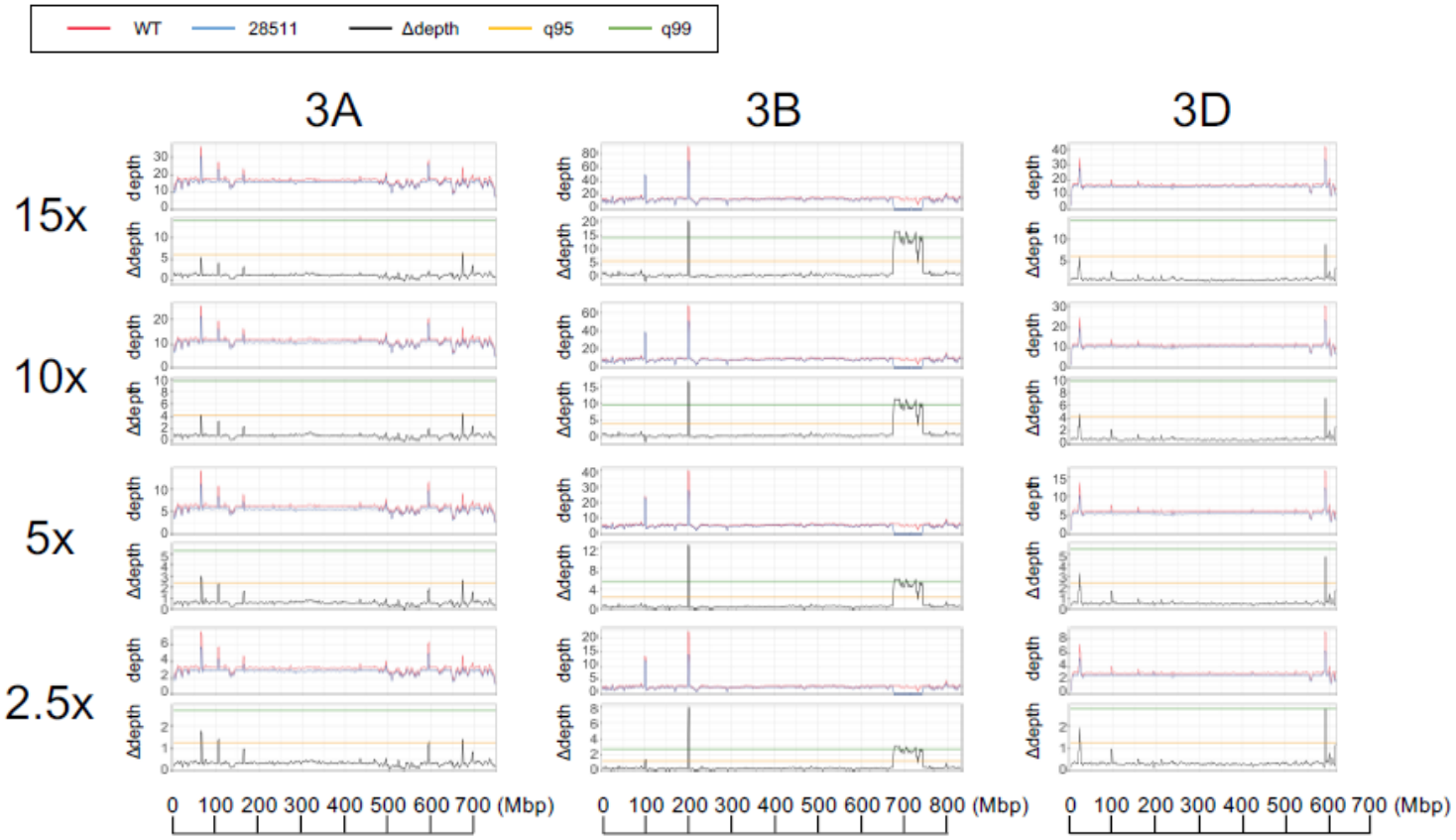

Figure 9

The tests of deletion detection power under different depth of coverage conditions Distribution of moving average of depth-of-coverage and difference of depth-of-coverage (Δdepth) between wild-type “Kitahonami” (WT) and the PHS-tolerant mutant “28511” on chromosome 3B under four depth coverage conditions: 15x, 10x, 5x, and 2.5x. are simulated. q95 and q99 indicate 95% and 99% confidence intervals, respectively. The number of reads of 15x, 10x, 5x, and 2.5x was described in Table 2.

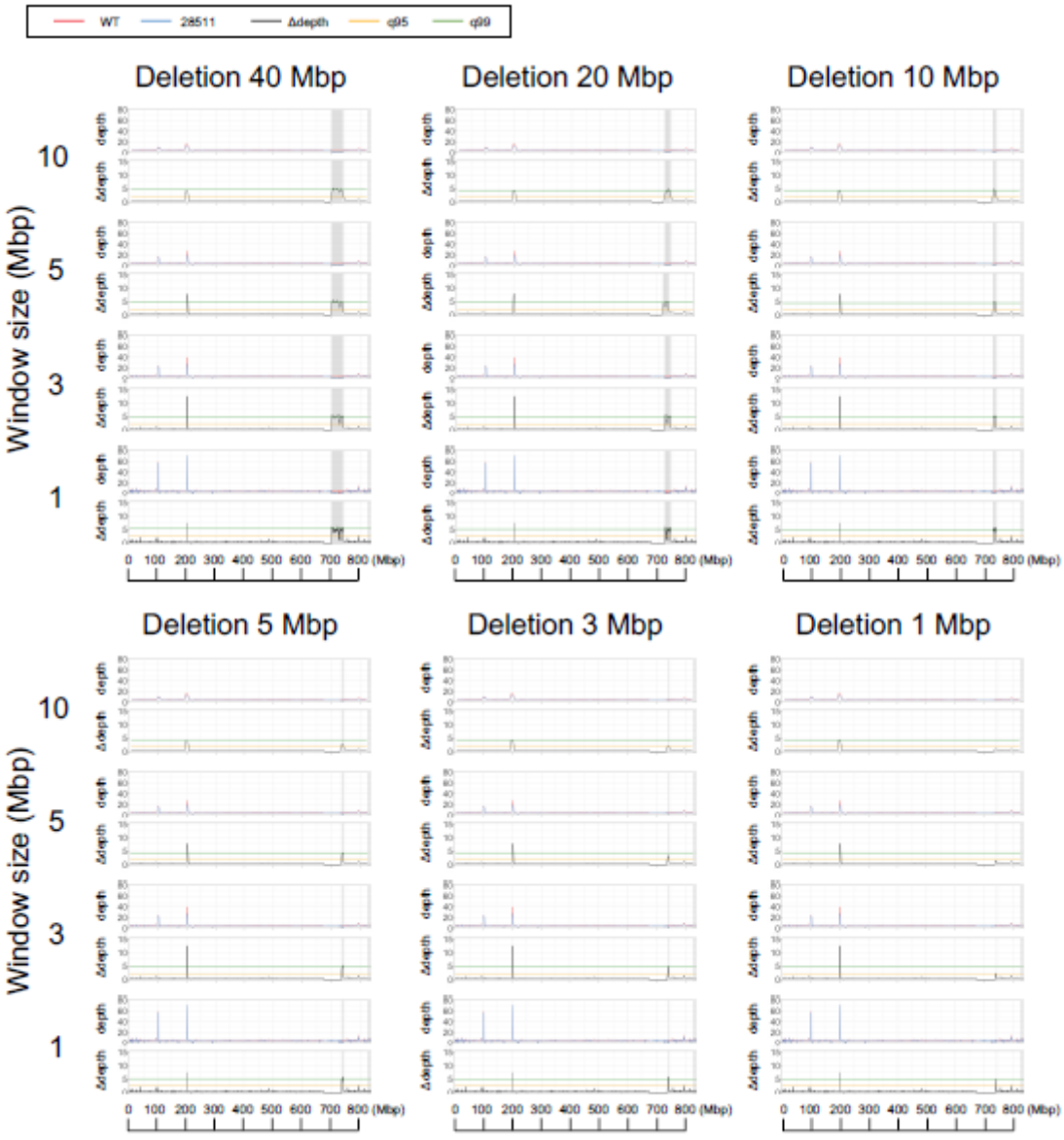

Figure 10

The tests of deletion detection power under different window sizes and different deletion sizes. Distribution of moving average of depth-of-coverage and difference of depth-of-coverage (Δdepth) between wild-type “Kitahonami” (WT) and the PHS-tolerant mutant “28511” under four window size conditions, 1 Mbp, 3 Mbp, 5 Mbp, and 10 Mbp, and six deletion sizes, 1 Mbp, 3 Mbp, 5 Mbp, 10 Mbp, 20 Mbp, and 40 Mbp, were simulated.

Figure 11

Distribution of SNPs between wild-type “Kitahonami” and the gamma-irradiated mutants over the chromosomes. A black line corresponds to one SNP location. G indicates the SNP distribution between wild-type “Kitahonami” and the grain hardness mutant “30579”. P indicates the SNP distribution between wild-type “Kitahonami” and the PHS-tolerant mutant “28511”.

Supplementary Files

This is a list of supplementary files associated with this preprint. Click to download.

- Additionalfile1.docx
- Additionalfile2.pdf